Geomechanics and Engineering, Vol. 1, No. 3 (2009) 205-218
DOI: http://dx.doi.org/10.12989/gae.2009.1.3.205

Bearing capacity factor N_γ for a rough conical footing

Vishwas N Khatri† and Jyant Kumar‡

Civil Engineering Department, Indian Institute of Science, Bangalore-560012, India

(Received November 18, 2008, Accepted July 16, 2009)

Abstract: The bearing capacity factor N_γ is computed for a rough conical footing placed over horizontal ground surface. The axisymmetric lower bound limit analysis formulation, in combination with finite elements and linear programming, proposed recently by the authors is used in this study. The variation of N_γ with cone apex angle (β), in a range of 30°-180°, is obtained for different values of ϕ; where ϕ is soil friction angle. For $\phi < 30°$, the magnitude of N_γ is found to decrease continuously with an increase in β from 30° to 180°. On the other hand, for $\phi > 30°$, the minimum magnitude of N_γ is found to occur generally between $\beta = 120°$ and $\beta = 150°$. In all the cases, it is noticed that the magnitude of N_γ becomes maximum for $\beta = 30°$. For a given diameter of the cone, the area of the plastic zone reduces generally with an increase in β. The obtained values of N_γ are found to compare quite well with those available in literature.

Keywords: axi-symmetry; bearing capacity; failure; limit analysis; optimization; plasticity.

1. Introduction

In recent years, a number of investigations have been performed on the determination of the bearing capacity factor N_γ for strip and circular footings. For strip footings, the solutions have been obtained mainly by using (i) the method of stress characteristics (Larkin 1968, Bolton and Lau 1993, Kumar 2003, 2009), (ii) the lower and upper bound finite element limit analysis (Ukritchon *et al.* 2003, Hjiaj *et al.* 2005, Lyamin *et al.* 2002, 2007, Kumar and Kouzer 2007, Kumar and Khatri 2008), (iii) the finite element method (Griffiths 1982), and (iv) FLAC (Frydman and Burd 1997). On the other hand, the available solutions for finding N_γ of circular footings have been obtained primarily by using the method of stress characteristics, in which case it is being assumed that the magnitude of the hoop stress (σ_θ) becomes equal to the minimum normal compressive stress (σ_3). For a flat smooth circular cylinder placed on a general c-ϕ soil, the solution for determining the magnitude of failure load on the basis of the method of stress characteristics was provided by Cox (1962). Further, Bolton and Lau (1993) and Martin (2004, 2005), computed N_γ for circular footings both with smooth and rough interfaces. For a rough footing base, due to an employment of a triangular (not curved) trapped wedge below the footing base, the N_γ values obtained by Bolton and Lau (1993) were found to be a little higher as compared to the solution of Martin (2004, 2005). By using FLAC, Erickson and Drescher (2002) have obtained the magnitude of N_γ for a rigid circular

† Research Scholar, E-mail: vishwas@civil.iisc.ernet.in
‡ Associate Professor, Corresponding author, E-mail: jkumar@civil.iisc.ernet.in

footing. With the usage of a three dimensional finite element limit analysis with non-linear programming, Lyamin *et al.* (2007) solved the problem of circular footings embedded in sand. Using the method of characteristics, Cassidy and Houlsby (2002) have provided the solution for finding the ultimate bearing capacity of conical footings placed on the surface of sand. In the present study, it is also intended to determine the collapse loads for conical footings placed on sand. The axi-symmetric lower bound limit analysis formulation presented earlier by the authors (Khatri and Kumar 2009) for $\phi = 0^o$ condition, and later extended by the authors (Kumar and Khatri 2009) for a general c-ϕ soil, is used in the present paper. The N_γ values are determined for various combinations of friction angles (ϕ) and cone apex angles (β). The effect of β on the plastic zones is also examined. The results obtained from the analysis are compared with those available in literature using different numerical methods.

2. Problem definition

A rigid conical footing with a rough base, and having an apex (interior) angle β, is placed on a homogeneous soil medium with horizontal ground surface. The footing is having radius b and is subjected to vertical downward load (Q) with its point of application coinciding with the vertical axis of the footing. It is prescribed that the footing is rigid and is subjected to vertical downward movement. The rigidity of the footing will ensure a uniform vertical displacement everywhere along the footing-soil interface; however, no attempt has been made in this study to incorporate exclusively the kinematics of the problem. The soil mass is assumed to be perfectly plastic, and it obeys an associated flow rule; Mohr-Coulomb's failure criterion is assumed to be applicable. It is required to determine the lower bound magnitude of the collapse load due to the component of soil unit weight (γ), for different combinations of β and ϕ.

3. Mesh details

Due to the symmetry about the vertical line passing through the centre of the footing, there is no need to consider the complete volumetric domain while solving the problem. Similar to a typical plane strain problem, the problem domain only in a r-z plane starting from $r = 0$ to $r = \infty$ has been considered like a very thin piece of pie; the parameters r and z refer to radial and vertical directions, respectively. The chosen domain and the associated stress boundary conditions are indicated in Fig. 1(a). The depth (d) of domain (refer Fig. 1a), was kept equal to L_g; where L_g is the horizontal extent of the chosen domain measured from the footing edge (point O in Fig. 1a). The values of L_g and d were computationally arrived by using a number of trials such that (i) the boundaries of the plastic zones, obtained from the analysis, were found to contain well within the boundaries of the chosen problem domain and (ii) the magnitude of the collapse load remains almost constant even if the size of the domain was further increased. The value of d is kept equal to (i) 5b for $\phi = 5^o$, and (ii) 26b for $\phi = 45^o$. The domain is discretized into a number of three noded triangular elements; the mesh is generated in a manner such that all the three sides of a given triangular element remain almost of the same size. The sizes of all the elements are gradually made smaller approaching towards the footing edge (point O in the Fig. 1a). Typical meshes chosen in the analysis for $\phi = 30^o$ and with different cone angles (β) are illustrated in Figs. 2-4; the parameters E, N, N_i and D_c in these figures

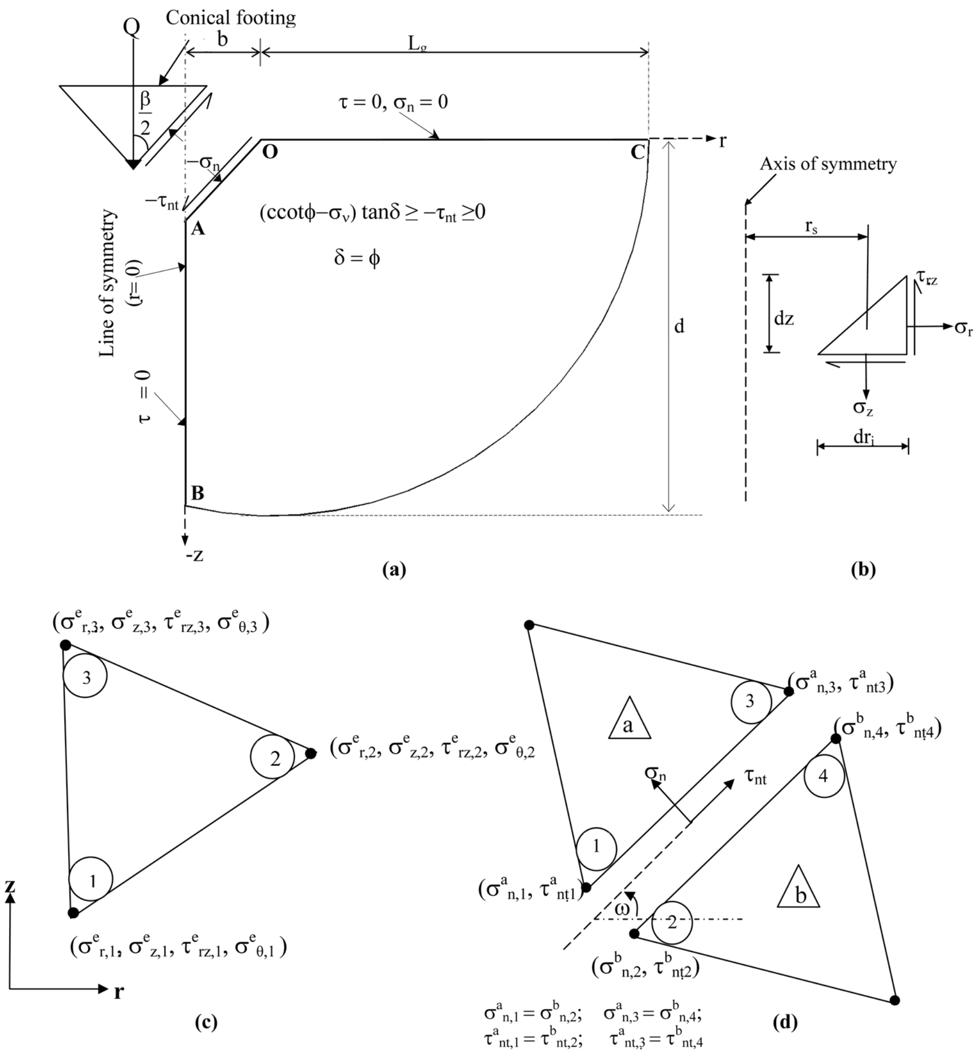

Fig. 1 (a) Problem domain and stress boundary conditions, (b) free body diagram of soil element along the cone base, (c) nodal stresses for a typical triangular element and (d) statically admissible stress discontinuity

refer to the total number of (i) elements, (ii) nodes, (iii) nodes along the footing-soil interface, and (iv) discontinuities, respectively.

4. Analysis

The axi-symmetric lower bound limit analysis formulation for $\phi = 0$ condition proposed earlier by authors (Khatri and Kumar 2009) and later extended to a general c-ϕ soil mass (Kumar and Khatri 2009) is used in the present article for carrying out the analysis. The axi-symmetric formulation proposed by the authors is simply a modification over the plane strain methodology presented

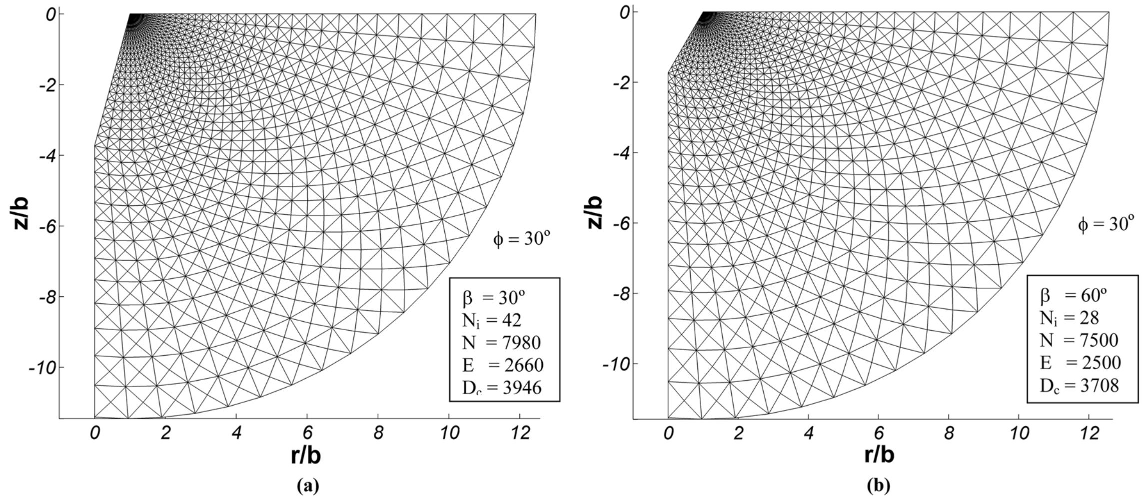

Fig. 2 Mesh used in the analysis for $\phi = 30^o$ with (a) $\beta = 30^o$ and (b) $\beta = 60^o$

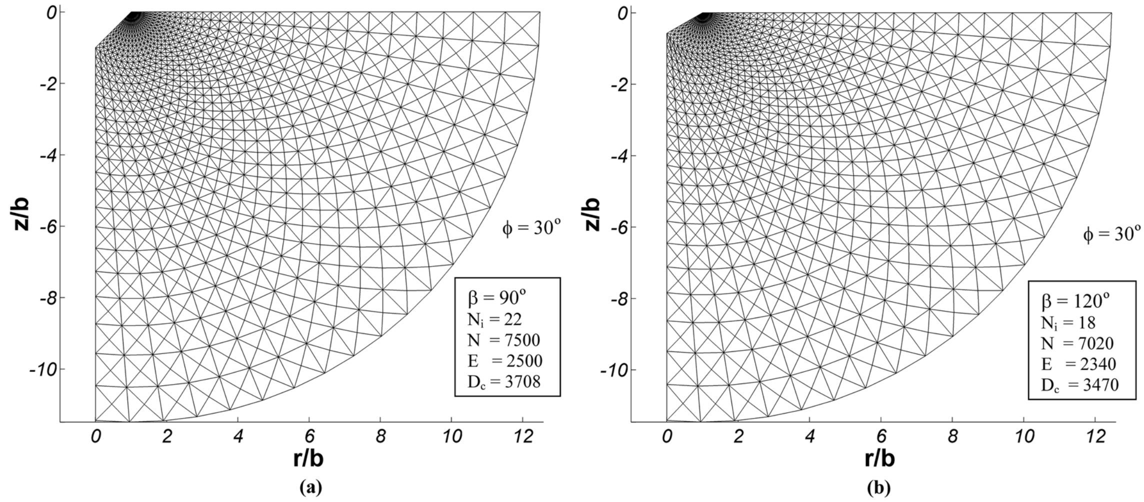

Fig. 3 Mesh used in the analysis for $\phi = 30^o$ with (a) $\beta = 90^o$ and (b) $\beta = 120^o$

earlier by Sloan (1988). The previous papers of the authors (Khatri and Kumar 2009, Kumar and Khatri 2009) can be referred for the necessary description about the method. A brief explanation is, however, provided here for the sake of completeness.

Nodal stresses (σ_r, σ_z, τ_{rz}, σ_θ) are treated as basic unknown variables. Three noded triangular elements are used to model the stress field as shown in Fig. 1(c). Statically admissible stress discontinuities, as illustrated in Fig. 1(d), are assumed along all the interfaces among adjacent triangles; at the interface of the two elements, the normal and shear stresses are assumed to be continuous. The basic expression for finding the magnitude of the total collapse load is generated from the integration of the stresses along the conical footing-soil interface on the basis of the satisfaction of the stress-boundary conditions, equilibrium equations and linearized yield criterion, along with additional inequality constraints arising from axi-symmetric formulation. The magnitude

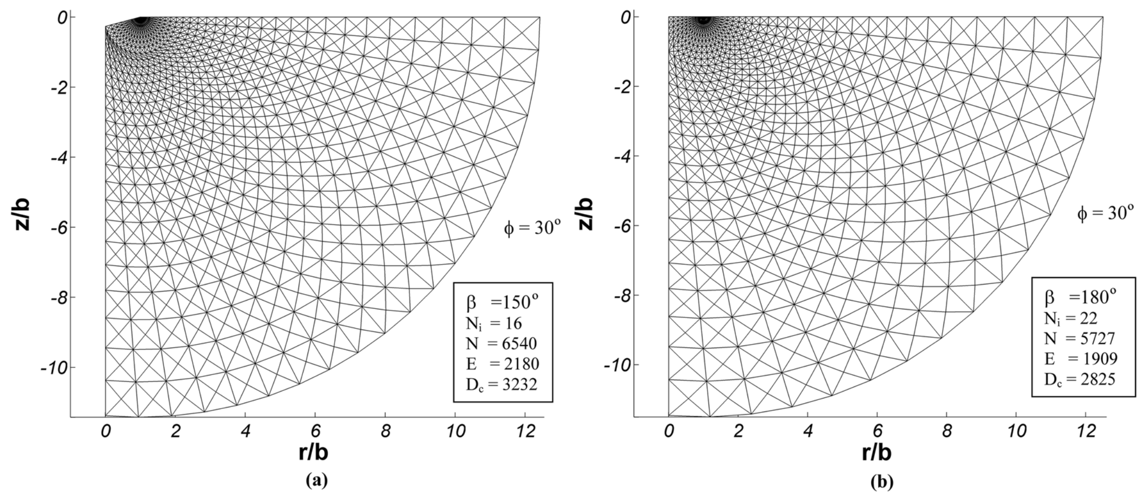

Fig. 4 Mesh used in the analysis for $\phi = 30°$ with (a) $\beta = 150°$ and (b) $\beta = 180°$

of the total collapse load is then maximized subjected to a number of equality and non-equality linear constraints on the nodal stresses.

The steps followed in this paper only associated with the yield condition exclusively for an axi-symmetric problem are described below.

4.1 Yield condition

Following Harr-Von Karman condition, the value of σ_θ (hoop stress) is specified close to σ_3 (least compressive normal stress) in a *r-z* plane for finding the ultimate bearing capacity of circular foundations. With the help of three additional inequality constraints arising from Fig. 5, this condition is specified. By drawing two Mohr circles having the common centre (that is, with $\sigma = (\sigma_r + \sigma_z)/2$), the admissible range of σ_θ (or σ_3) is achieved, as shown in Fig. 5. The larger circle corresponds to at yield and, therefore, it touches the Mohr-Coulomb yield line AF. Whereas, the smaller circle represents the possible state of stress at a point in the r-z plane with given values of σ_r, σ_z and τ_{rz}. On this basis, the possible location of the point E (associated with least compressive normal stress (σ_3) for the smaller circle) can vary between points G (greater of σ_r and σ_z) and H (σ_{3f} associated with larger circle). In order that the value of σ_θ remains closer to σ_3, following three inequality constraints are arrived:

$$\sigma_{\theta,i} \ge \sigma_{r,i}$$

$$\sigma_{\theta,i} \ge \sigma_{z,i}$$

$$\sigma_{\theta,i} \le \sigma_{3f,i}$$

where, $\sigma_{\theta,i}$, $\sigma_{r,i}$, $\sigma_{z,i}$ are the nodal stresses associated with node *i* and $\sigma_{3f,i}$ is the minor principal stress (least compressive normal stress) at failure. These constraints are expressed in the matrix form as,

$$[A^i_{s\theta}]_{3\times 4}\{\theta^i\}_{4\times 1} \le \{b^i_{s\theta}\}_{3\times 11} \quad (1)$$

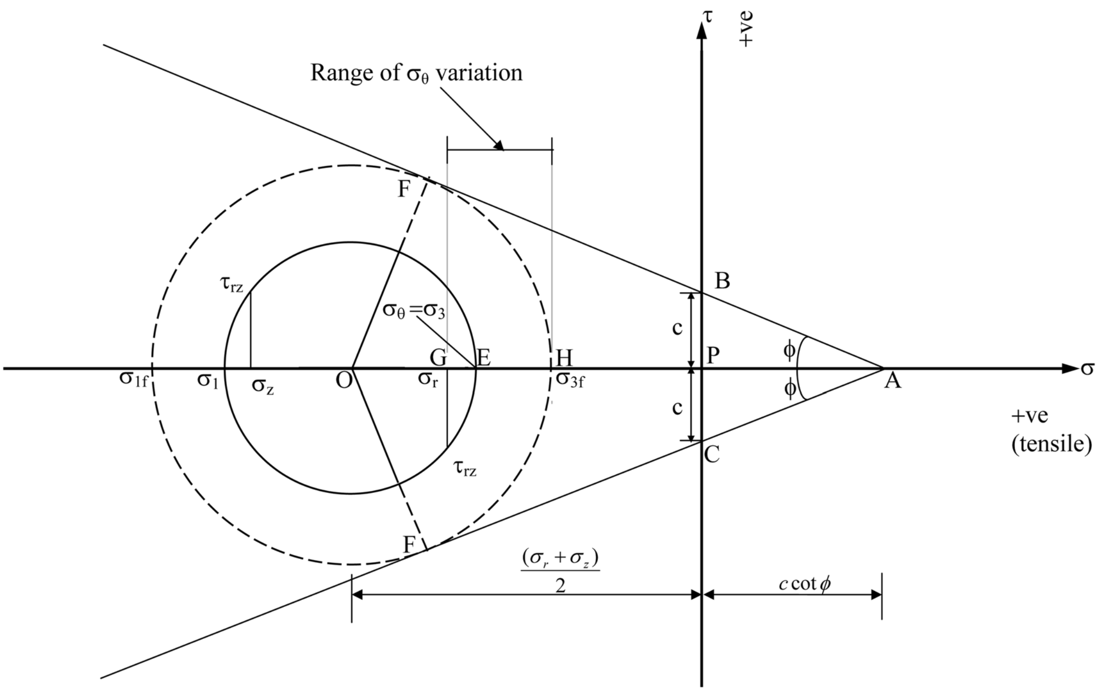

$$\sigma_{3f} = \frac{(\sigma_r + \sigma_z)}{2} + \left\{ -\frac{(\sigma_r + \sigma_z)}{2} + c\cot\phi \right\} \sin\phi$$

Fig. 5 The possible range for the variation of σ_θ

where, $$[A^i_{s\theta}]_{3\times 4} = \begin{bmatrix} 1 & 0 & 0 & -1 \\ 0 & 1 & 0 & -1 \\ -\frac{(1-\sin\phi)}{2} & -\frac{(1-\sin\phi)}{2} & 0 & 1 \end{bmatrix}$$

$$\{\sigma^i\}^T_{4\times 1} = \{\sigma_{r,i}\ \sigma_{z,i}\ \sigma_{rz,i}\ \sigma_{\theta,i}\}_{1\times 4}$$

$$\{b^i_{s\theta}\}^T_{3\times 1} = \{0\ 0\ c\cos\phi\}$$

To ensure that the finite element formulation leads to a linear programming problem, the Mohr-Coulomb yield surface is approximated by a regular polygon of p sides inscribed to the parent yield surface (Bottero *et al.* 1980). Following linearized inequality condition needs to be specified in order that the stress state does not violate the yield condition:

$$A_k\sigma_r + B_k\sigma_z + C_k\tau_{rz} \le \mathrm{D}; \qquad k = 1, 2, \ldots, p. \tag{2}$$

where,

$$A_k = \cos(2\pi k/p) + \sin\phi\cos(\pi/p),\ B_k = \sin\phi\cos(\pi/p) - \cos(2\pi k/p),$$
$$C_k = 2\sin(2\pi k/p), \qquad D = 2c\cos\phi\cos(\pi/p) \tag{3}$$

The inequality constraints imposed on four stresses at node i, due to linearized yield criterion will become p in number.

4.2 Objective function

The soil element immediately along the cone base is shown in Fig. 1(b). The magnitude of the collapse load (objective function) is obtained by numerical integrating the stresses over the complete area of the conical footing-soil interface, as given by the following expression:

$$Q = -\sum_{i=1}^{s} [\sigma_z r_s dr_i - \tau_{rz}(r_s + 0.5dr_i)dz_i](2\pi) \quad (4)$$

where, s = no of boundary edges chosen along the soil-footing interface, r_s = distance measured from axis of symmetry to the midpoint of a particular i[th] element; dr_i and dz_i are defined in Fig. 1(b). Since the stresses are assumed to vary linearly throughout each element, the magnitude of σ_z and τ_{rz} in the above expression is replaced as,

$$\sigma_z = \frac{(\sigma_{z1} + \sigma_{z2})}{2} \text{ and } \tau_{rz} = \frac{(\tau_{rz1} + \tau_{rz2})}{2} \quad (5)$$

where, σ_{z1}, σ_{z2} and τ_{rz1}, τ_{rz2} are stresses at the two boundary nodes 1 and 2. After substituting for σ_z and τ_{rz} Eq. (4) can be written in the matrix form as,

$$Q_s = \{g^s\}^T_{1\times 8}\{\sigma^s\}_{8\times 1} \quad (6)$$

$$\{g^s\}^T = \{0\ -\pi r_s dr_i\ \ \pi dz_i(r_s + 0.5dr_i)\ 0\ 0\ -\pi r_s dr_i\ \ \pi dz_i(r_s + 0.5dr_i)\ 0\}_{1\times 8}$$

$$\{\sigma^s\}^T = \{\sigma^s_{r,1}\ \sigma^s_{z,1}\ \sigma^s_{rz,1}\ \sigma^s_{\theta,1}\ \sigma^s_{r,2}\ \sigma^s_{z,2}\ \sigma^s_{rz,2}\ \sigma^s_{\theta,2}\}_{1\times 8}$$

It should be noted that, for a flat circular footing ($\beta = 180°$), the shear stress terms in Eq. (5) will simply vanish since $dz_i = 0$.

The formulation of the lower bound limit analysis is stated in the form of standard linear programming problem:

$$\text{Maximize } \{g\}^T\{\sigma\} \quad (7a)$$

$$\text{Subject to } [A_1]\{\sigma\} = \{b_1\} \quad (7b)$$

$$[A_2]\{\sigma\} \le \{b_2\} \quad (7c)$$

where, $\{\sigma\}$ is a vector of nodal stresses given by

$$\{\sigma\}^T = [\sigma_{r,1}\ \sigma_{z,1}\ \tau_{rz,1}\ \sigma_{\theta,1}\ \sigma_{r,2}\ \sigma_{z,2}\ \tau_{rz,2}\ \sigma_{\theta,2}\ \ldots\ \ldots\ \sigma_{r,N},\ \sigma_{z,N}\ \tau_{rz,N}\ \sigma_{\theta,N}]$$

The solution of this optimization problem, gives statically admissible stress field $\{\sigma\}$ and collapse load $\{g\}^T\{\sigma\}$. For the present problem, the magnitude of the compressive load needs be maximized. On lines similar with Kumar and Kouzer (2007) and Kumar and Khatri (2008), the linear optimization is carried out by using "LINPROG" a library program in MATLAB.

5. Definition of N_γ

After obtaining the magnitude of the collapse load (Q), the bearing capacity factor N_γ is defined by using the following expression:

$$\frac{Q}{\pi b^2} = 0.5(2b)\gamma N_\gamma \quad (8)$$

It needs to be mentioned that the magnitude of the collapse load (Q) in the above expression implies the total load which the footing base can impose on soil media; therefore, Q will comprise of the summation of the weight of the footing (conical base) itself and the load exerted on the top of the footing.

6. Results and comparisons

The computations were performed for different values of (i) β ranging from 30º to 180º, and (ii) ϕ varying from 5º to 45º. The value of p is kept equal to 21. The results from the analysis are summarized herein:

6.1 The variation of N_γ with β

The variation of N_γ for different combinations of ϕ and β is provided in Table 1. These results are also presented in Fig. 6; in this figure, in order to provide a comparison, the computational results of Cassidy and Houlsby (2002) on the basis of the method of stress characteristics have also been included. It can be noted that for $\phi < 30$º, the magnitude of N_γ reduces continuously with an increase in cone angle (β) and a flat circular footing ($\beta = 180$º) provides always the minimum value of N_γ. However, for $\phi > 30$º, the minimum magnitude of N_γ occurs somewhere between the value of β equal to 120º and 150º. For the entire chosen range of ϕ, the cone with an apex angle of 30º, always provides the maximum values of N_γ; the computations, however, were not performed for $\beta < 30$º. The obtained results in all the cases compare quite well with those given by Cassidy and Houlsby (2002); the present N_γ values were found to be generally very slightly lower.

6.2 The comparison of N_γ for a flat circular footing (β = 180º)

For a flat circular rough footing ($\beta = 180$º), an exclusive comparison of the values of N_γ obtained

Table 1 The variation of N_γ with β for different values of ϕ as obtained from the present analysis for a rough cone base

ϕ	βº					
	30	60	90	120	150	180
5	2.67	1.08	0.62	0.38	0.22	0.08
10	5.38	2.00	1.15	0.76	0.51	0.3
15	10.55	3.76	2.19	1.53	1.16	0.88
20	20.73	7.17	4.31	3.18	2.63	2.27
25	41.53	14.37	8.85	6.88	6.1	5.68
30	86.04	30.28	19.34	15.74	14.6	14.65
35	189.07	68.62	45.82	38.92	37.2	39.97
40	455.42	170.91	120.06	108.14	106.28	116.2
45	1225.4	490.33	364.72	341.24	343.44	379.79

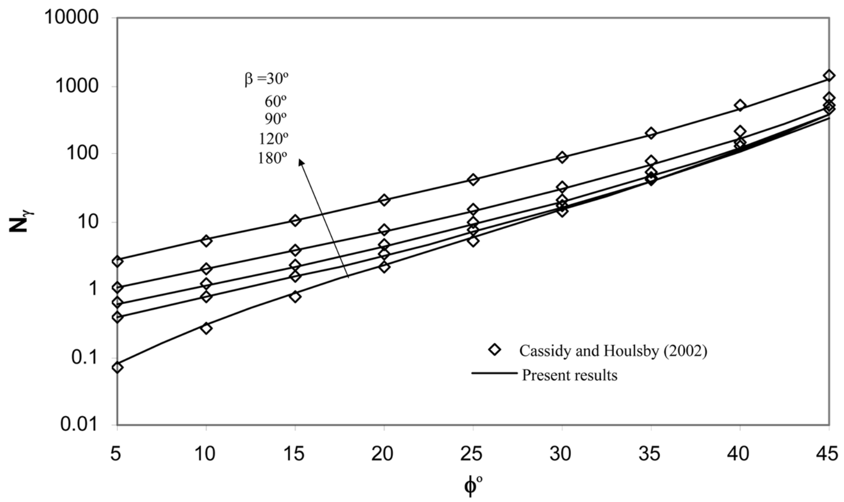

Fig. 6 A comparison of N_γ values obtained from the present analysis with those published by Cassidy and Houlsby (2002)

Table 2 A comparison of N_γ values for a rough circular footing

ϕ^o	Present method ($\delta = \phi$)	Martin (2004, 2005)	Erickson and Drescher (2002)	Krabbenhoft *et al.* (2008)	Lyamin *et al.* (2007)
				Lower bound	Lower bound
	a	b	c	d	d
5	0.08	0.08	-	-	-
10	0.30	0.32	-	0.31	-
15	0.88	0.93	-	-	-
20	2.27	2.41	2.80	2.26	-
25	5.68	6.07	-	-	5.65
30	14.65	15.54	-	13.98	14.10
35	39.97	41.97	45.00	-	37.18
40	116.20	124.10	130.00	108.46	106.60
45	379.79	419.44	456.00	-	338.00

a: Lower bound limit analysis with finite elements and linear programming
b: Method of characteristics
c: By using FLAC
d: Three dimensional numerical limit analysis with finite elements and non-linear programming

from the present analysis was made with the results given by (i) Martin (2004, 2005) based on the method of characteristics, (ii) Lyamin *et al.* (2007) and Krabbenhøft *et al.* (2008) by using a rigorous three dimensional finite element lower bound limit analysis, and (iii) Erickson and Drescher (2002) using FLAC. The comparison of all these results is provided in Table 2. It can be seen that the present N_γ values are slightly smaller than those obtained with the method of stress characteristics. The lower bound values of N_γ provided by Lyamin *et al.* (2007) and Krabbenhøft *et al.* (2008) were found to be very close to the present solution; the present N_γ values were generally noted to be very marginally greater (better lower bound solution) than those given by Lyamin *et al.* (2007) and Krabbenhøft *et al.* (2008).

It should be mentioned that N_γ values presented in this paper become exactly the same as those given by the authors for a flat circular foundation (Kumar and Khatri 2009). In the companion paper of Kumar and Khatri (2009), the computational results are obtained for a general c-ϕ soil but only with a flat circular foundation base ($\beta = 180^\circ$, not for a conical base) for smooth as well as rough footing-soil interface.

6.3 Plastic zones

In case if the Mohr circle associated with a given state of stress touches the failure envelope, the point will be in a state of shear failure. In the present case, the states of all elements with reference to the shear failure, at their respective centroids, were defined in terms of a ratio, a/d; where

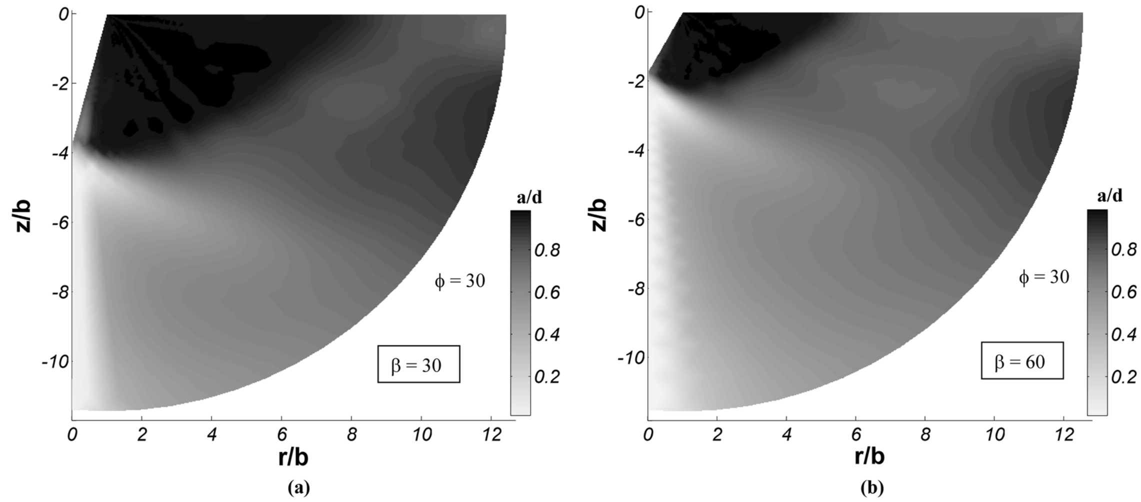

Fig. 7 Plastic zones obtained from the analysis for $\phi = 30^\circ$ with (a) $\beta = 30^\circ$ and (b) $\beta = 60^\circ$

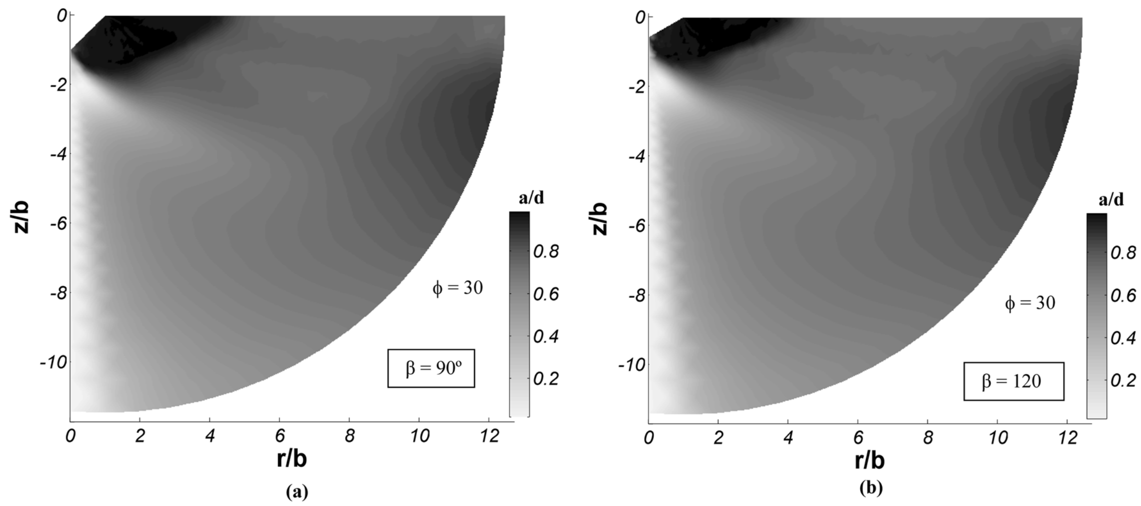

Fig. 8 Plastic zones obtained from the analysis for $\phi = 30^\circ$ with (a) $\beta = 90^\circ$ and (b) $\beta = 120^\circ$

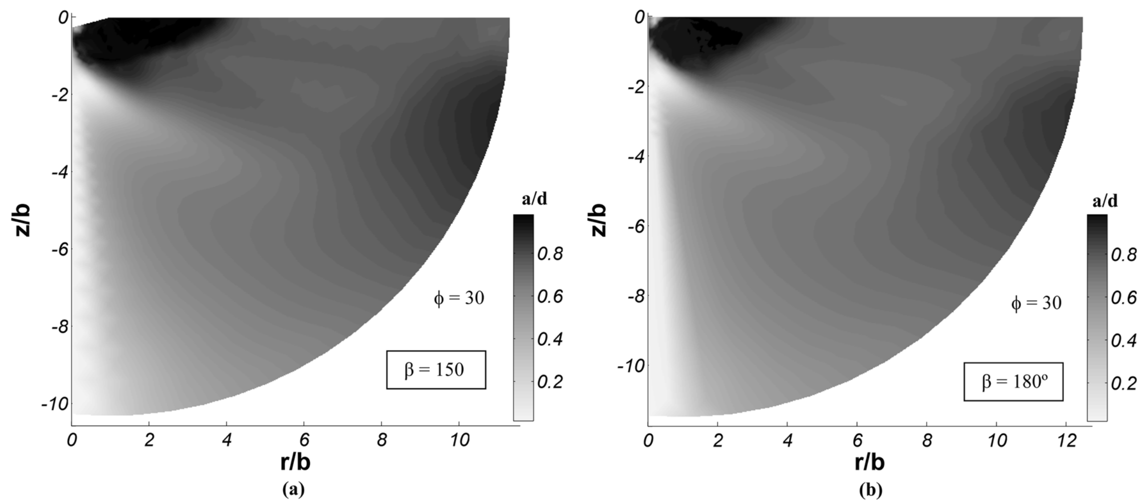

Fig. 9 Plastic zones obtained from the analysis for $\phi = 30^o$ with (a) $\beta = 150^o$ and (b) $\beta = 180^o$

$a = (\sigma_r - \sigma_z)^2 + (2\tau_{rz})^2$, and $d = [2c\ \cos\phi - (\sigma_r + \sigma_z)\sin\phi]^2$; cohesion, $c = 0$ in the present case. If $a/d <$ 1, it will indicate that the point will be in a non-plastic state. On the other hand, if the value of a/d becomes equal to 1, the point will be in a state of shear failure. In this manner, the plastic zones were obtained for different values of β. The plastic zones for the different cases, with $\phi = 30^o$, are illustrated in Figs. 7-9; the plastic zones are drawn in a manner such that the color of an element becomes continuously darker when approaching towards the shear failure ($a/d = 1$). It can be noticed that a very dark zone exists everywhere around the footing base. This dark zone indicates the region of the plastic failure in the soil mass. It can be noticed that the area of the plastic zone, with respect to a given diameter of the footing, decreases generally in a continuous fashion with an increase in the value of β; the size of the plastic zone becomes maximum for $\beta = 30^o$. It can further be noticed as the value of β was increased a small non-plastic zone was noticed below the footing base; a non-plastic wedge around the footing base is clearly noticed for $\beta = 180^o$.

7. Remarks

7.1 The effect of extension elements on N_γ

In order to ensure that the obtained lower bound solution nowhere violates the yield condition within the domain the boundaries of which are extended even up to infinity, additional inequality constraints arising from the yield condition are imposed on the elements, named extension elements, lying on the chosen boundary of the problem domain. Typical chosen meshes with the inclusion of 3-noded extension elements for $\phi = 30^o$ with three different values of β, namely, 30°, 90° and 150°, are illustrated in Fig. 10; the term E_{ext} in these figures refer to the number of extension elements used in the chosen mesh. In this figure, for a chosen extension element (shown with grey shade), the directions of boundary extensions towards infinity are also indicated; the edges 5-6 and 11-12 in Fig. 10c point towards the directions of extension. To extend the stress field up to infinity, following additional inequality constraints were imposed on extension nodes (5, 6 and 11, 12),

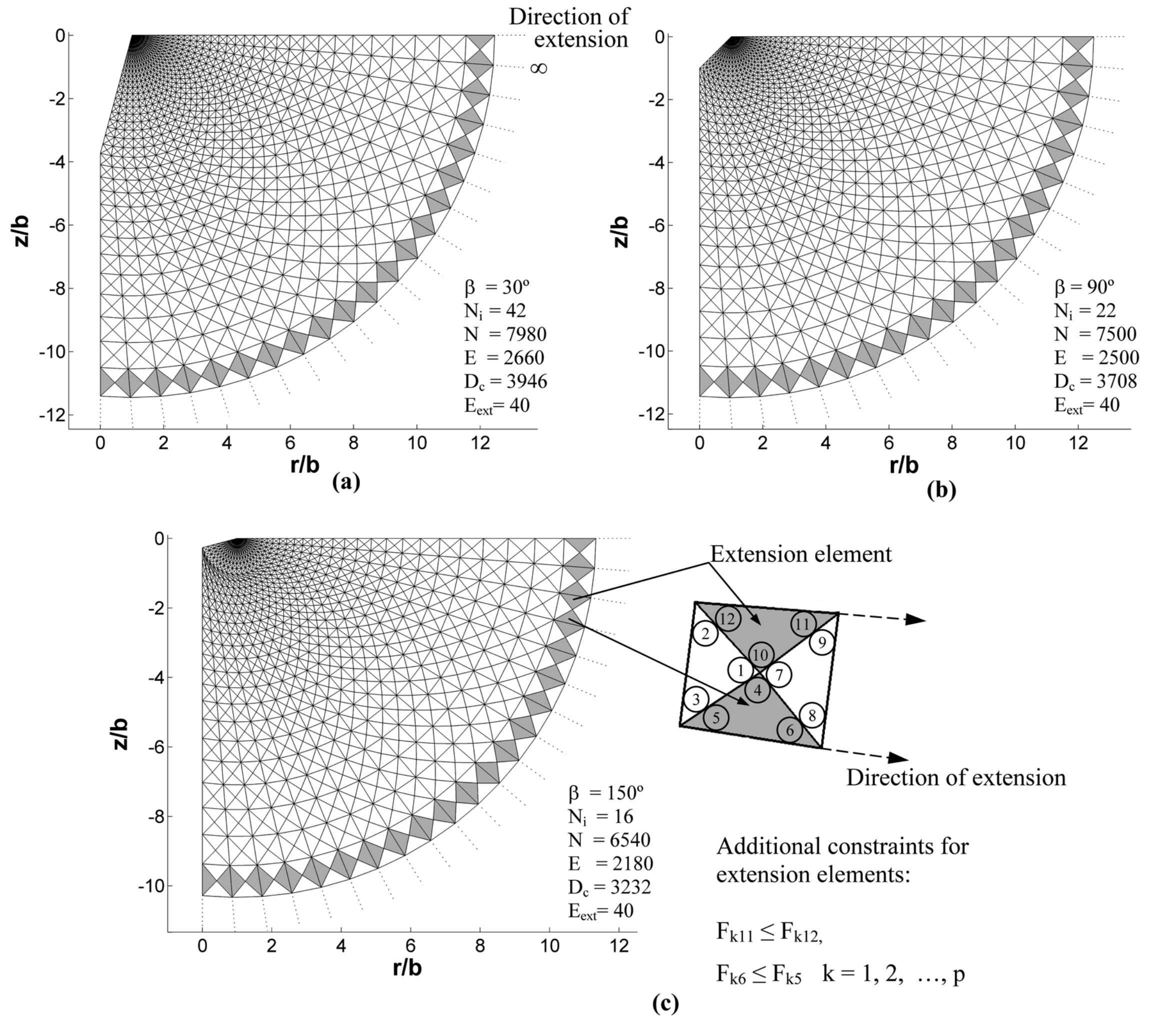

Fig. 10 The chosen meshes with extension elements for $\phi = 30^{\circ}$ with (a) $\beta = 30^{\circ}$, (b) $\beta = 90^{\circ}$ and (c) $\beta = 150^{\circ}$

$$F_{k6} - F_{k5} \leq 0 \quad k = 1, 2, 3, \ldots\ldots\ldots\ldots, p \tag{10}$$

$$F_{k11} - F_{k12} \leq 0 \quad k = 1, 2, 3, \ldots\ldots\ldots\ldots, p \tag{11}$$

where, $F_{ki} = A_k\sigma_{ri} + B_k\sigma_{zi} + C_k\tau_{rzi} - D$; $k = 1, 2, \ldots, p$, the terms A_k, B_k, C_k and D are already defined earlier by Eq. (3). The reference of Ukritchon (1996) can be refereed for the derivations of the above constraints imposed on the extension elements. The subscript i in the above equation corresponds to the extension node number. All the other equality and inequality constraints including those on the hoop stress (σ_θ), remain unchanged on the extension elements. Typical numerical results with and without the inclusion of extension elements for $\phi = 30^{\circ}$ and with $\beta = 30^{\circ}$-180° are given in Table 3. It can be seen that the N_γ values obtained with and without the usage of extension elements remain very much close to each other. This observation is on account of fact that the chosen size of domain is adequately large and all the yielded elements are contained quite well within the periphery of the chosen domain. With the incorporation of additional constraints on

Table 3 A comparison of N_γ values with and without the inclusion of extension elements for a rough cone base with $\phi = 30°$

Apex angle ($\beta°$)	N_γ	
	Without extension elements	With extension elements
30	86.0441	86.0433
60	30.2823	30.2819
90	19.345	19.345
120	15.7428	15.7427
150	14.5991	14.5990
180	14.6453	14.6451

extension elements a very slight reduction in the magnitude of collapse load is noted. The comparison of N_γ values with and without the use of extension elements suggests that the results presented earlier will not be significantly different from the values of N_γ values even with the usage of extension elements.

8. Conclusions

By using a lower bound limit analysis in combination with finite elements and linear programming, the bearing capacity factor N_γ is computed for a conical footing with a rough base. It is noticed that the magnitude of N_γ increases generally with a decrease in the apex (interior) angle of the cone. This implies that for a given diameter of the footing, with respect to the shear failure consideration, it will be generally advantageous to employ a conical footing with an acute apex angle rather than simply using a flat circular footing. The obtained results in all the cases were found to be generally very close to those available in literature by using the method of stress characteristics.

References

Bolton, M.D. and Lau, C.K. (1993), "Vertical bearing capacity factors for circular and strip footings on Mohr-Coulomb soil", *Can. Geotech. J.*, **30**(6), 1024-1033.

Bottero, A., Negre, R., Pastor, J. and Turgeman, S. (1980), "Finite element method and limit analysis theory for soil mechanics problem", *Comput. Method. Appl. M.*, **22**(1), 131-149.

Cassidy, M.J. and Houlsby, G.T. (2002), "Vertical bearing capacity factors for conical footings on sand", *Geotechnique*, **52**(9), 687-692.

Cox, A.D. (1962), "Axially symmetric plastic deformation in soils-II. Indentation of Ponderable soils", *Int. J. Mech. Sci.*, **4**, 371-380.

Erickson, H.L. and Drescher, A. (2002), "Bearing capacity of circular footings", *J. Geotech. Geoenviron.*, **128**(1), 38-43.

Frydman, S. and Burd, H.J. (1997), "Numerical studies of bearing capacity factor N_γ", *J. Geotech. Geoenviron.*, **123**(1), 20-29.

Griffiths, D.V. (1982), "Computations of bearing capacity factors using finite elements", *Geotechnique*, **32**(3), 195-202.

Hjiaj, M., Lyamin, A.V. and Sloan, S.W. (2005), "Numerical limit analysis solutions for the bearing capacity factor N_γ", *Int. J. Solids Struct.*, **42**(5-6), 1681-1704.

Krabbenhøft, K., Lyamin, A.V. and Sloan, S.W. (2008), "Three-dimensional Mohr-Coulomb limit analysis using semi-definite programming", *Commun. Numer. Meth. En.*, **24**(11), 1107-1119.

Kumar, J. (2003), "N_γ for rough strip footing using the method of characteristics", *Can. Geotech. J.*, **40**(3), 669-674.

Kumar, J. (2009), "The variation of N_γ with footing roughness using the method of characteristics", *Int. J. Numer. Anal. Met. Geomech.*, **33**(2), 275-284.

Kumar, J. and Kouzer, K.M. (2007), "Effect of footing roughness on bearing capacity factor N_γ", *J. Geotech. Geoenviron.*, **133**(5), 502-511.

Kumar, J. and Khatri, V.N. (2008), "Effect of footing roughness on lower bound N_γ values", *Int. J. Geomech.*, **8**(3), 176-187.

Kumar, J. and Khatri, V.N. (2009), "Bearing capacity factors of circular foundations for a general c-ϕ soil using lower bound finite element limit analysis", *Int. J. Numer. Anal. Met.*

Khatri, V.N. and Kumar, J. (2009), "Bearing capacity factor N_c under $\phi = 0$ condition for piles in clays", *Int. J. Numer. Anal. Met. Geomech.*, **33**(9), 1203-1225.

Larkin, L.A. (1968), "Theoretical bearing capacity of very shallow footings", *J. Soil Mech. Found. Engng. Div.*, ASCE, **94**(6), 1347-1357.

Lyamin, A.V. and Sloan, S.W. (2002), "Lower bound limit analysis using non-linear programming", *Int. J. Numer. Meth. Eng.*, **55**, 573-611.

Lyamin, A.V., Salgado, R., Sloan, S.W. and Prezzi, M. (2007), "Two and three-dimensional bearing capacity of footings in sand", *Geotechnique*, **57**(8), 647-662.

Martin, C.M. (2004), ABC-Analysis of Bearing Capacity. Available online from www-civil.eng.ox.ac.uk/people/cmm/software/abc 2004.

Martin, C.M. (2005), "Exact bearing capacity calculations using the method of characteristics", *Proceedings of the 11th IACMAC, Torino, June*, 441-450.

Sloan, S.W. (1988), "Lower bound limit analysis using finite elements and linear programming", *Int. J. Numer. Anal. Met.*, **12**, 61-77.

Sloan, S.W. and Kleeman, P.W. (1995), "Upper bound limit analysis using discontinuous velocity fields", *Comput. Method. Appl. M.*, **127**(1), 293-314.

Ukritchon, B. (1996), *Evaluation of numerical limit analyses by finite elements and linear programming*, M.Sc. thesis, Massachusetts Institute of Technology.

Ukritchon, B., Whittle, A.W. and Klangvijit, C. (2003), "Calculation of bearing capacity factor N_γ using numerical limit analysis", *J. Geotech. Geoenviron.*, ASCE, **129**(7), 468-474.